https://doi.org/10.5194/egusphere-2023-1102
Preprint. Discussion started: 30 May 2023

Bulk and molecular-level composition of primary organic aerosol from wood, straw, cow dung, and plastic burning

Jun Zhang[1], Kun Li[1,a], Tiantian Wang[1], Erlend Gammelsæter[1,b], Ka Yuen Cheung[1], Mihnea Surdu[1], Sophie Bogler[1], Deepika Bhattu[2], Dongyu S. Wang[1], Tianqu Cui[1], Lu Qi[1], Houssni Lamkaddam[1], Imad El Haddad[1], Jay G. Slowik[1], Andre S. H. Prevot[1], David M. Bell[1]

[1]Laboratory of Atmospheric Chemistry, Paul Scherrer Institute, Villigen, 5232, Switzerland

[2]Department of Civil and Infrastructure Engineering, Indian Institute of Technology Jodhpur, 342037, India

[a]now at: Environmental Research Institute, Shandong university, Qingdao, 266237, China

[b]now at: Department of Chemistry, Norwegian University of Science and Technology, Trondheim, 7491, Norway

Correspondence to: Andre S. H. Prevot (andre.prevot@psi.ch) and David M. Bell (david.bell@psi.ch)

Abstract. During the past decades, the source apportionment of organic aerosol (OA) in the ambient air has been improving substantially. The database of source retrieval model resolved mass spectral profiles for different sources has been built with the aerosol mass spectrometer (AMS). However, distinguishing similar sources (such as wildfires and residential wood burning) remains challenging, as the hard ionization of AMS mostly fragments compounds and therefore cannot capture the detailed molecular information. Recent mass spectrometer technologies of soft ionization and high mass resolution have allowed for aerosol characterization at the molecular formula level. In this study, we systematically estimated the emission factors and characterized the primary OA (POA) chemical composition with the AMS and the extractive electrospray ionization time-of-flight mass spectrometer (EESI-TOF) for the first time from a variety of solid fuels, including beech logs, spruce and pine logs, spruce and pine branches and needles, straw, cow dung, and plastic bags. The emission factors of organic matter and hydrocarbon gases are 16.2 ± 10.8 g kg^{-1} and 30.3 ± 8.5 g kg^{-1} for cow dung burning, which is generally higher than that of wood (beech, spruce, and pine), straw, and plastic bags burning (in the range from 1.3 to 6.2 g kg^{-1} and 2.8 to 9.4 g kg^{-1}). The POA measured by the AMS shows that the f_{60} (mass fraction of *m/z* 60) varies from 0.003 to 0.04 based on fuel types and combustion efficiency for wood (beech, spruce, and pine) and cow dung burning. The contribution of some polycyclic aromatic hydrocarbons is linked to burning fuels. On molecular level, the dominant compound of POA from wood, straw, and cow dung is $C_6H_{10}O_5$ (mainly levoglucosan), contributing ~7% to ~30% of the total intensity, followed by $C_8H_{12}O_6$ with fractions of ~2% to ~9%. However, as they are prevalent in all burns of biomass material, they cannot act as tracers for the specific sources. By using the Mann-Whitney U test among the studied fuels, we find specific potential new markers for these fuels from the measurement of the AMS and EESI-TOF. Markers from spruce and pine burning could be resin and conifer needle-related. The product from pyrolysis of hardwood lignins is found especially in beech logs burning. Nitrogen-containing species are selected markers primarily for cow dung open burning. These markers provide important support for the source apportionment.

Key words: AMS, EESI-TOF, biomass burning, source apportionment, markers

https://doi.org/10.5194/egusphere-2023-1102
Preprint. Discussion started: 30 May 2023

1 Introduction

Emissions from combustion are a major source of primary organic aerosol (POA), black carbon (BC), inorganic aerosol, and inorganic / organic gases (Andreae, 2019; Bond et al., 2007). After being emitted to the atmosphere, volatile organic compounds (VOCs) can further react to form lower volatility components and generate secondary organic aerosol (SOA). The primary emissions and their subsequent transformations have significant implications for air quality, climate, and human health (Chen et al., 2017). Accordingly, a large number of laboratory and field measurements have been carried out to disentangle the roles of burning-induced aerosols in polluted areas.

Solid fuel combustion is a major source of air pollution in many places over the world. In Southeast Asia, haze events are mainly attributed to the wildfires, agricultural waste burning, and peatland fires (Adam et al., 2021). In developing regions, such as India, more than half of households use inefficient stoves for cooking, burning solid fuels such as firewood, charcoal, crop residues and cow dung (Census of India, 2011). This contributes to poor household air quality, chronic and acute respiratory diseases, and even premature death (Smith et al., 2014). The extent to which primary particulate matter adversely affects health is source-dependent. Recent studies have shown that biomass burning-related particles has been linked to reactive oxygen species and oxidative stress, increasing the risks of cardiovascular diseases (Daellenbach et al., 2020; De Oliveira Alves et al., 2017; Tuet et al., 2019). Therefore, identifying the sources of aerosols is essential for assessing health risks and developing mitigation strategies.

Organic aerosol (OA) source apportionment has been widely studied using receptor models, e.g. positive matrix factorization (PMF), with OA composition characterized by an aerosol mass spectrometer (AMS) or aerosol chemical speciation monitor (ACSM). Many studies have successfully resolved source-related factors, for example, hydrocarbon-like OA (HOA), oxygenated OA (OOA), biomass burning OA (BBOA), coal combustion OA (CCOA), and so on, via PMF (Chen et al., 2021; Huang et al., 2014; Ng et al., 2010; Tobler et al., 2020; Wang et al., 2019; Crippa et al., 2014). The identification and validation of resolved factors rely strongly upon the spectral characteristics of source emissions. For example, hydrocarbon ion series $C_nH_{2n+1}^+$ and $C_nH_{2n-1}^+$, e.g. $C_4H_9^+$ at *m/z* 57 and $C_3H_5^+$ at *m/z* 41, are often referenced as tracers for HOA (Mohr et al., 2012), while $C_2H_4O_2^+$ at *m/z* 60 is the main marker for wood and other biomass burning, as $C_2H_4O_2^+$ is a characteristic major fragment of anhydrosugars (e.g. levoglucosan) produced from cellulose pyrolysis (Alfarra et al., 2007). However, achieving finer separation and interpretation of sources within one of the OA categories mentioned above from highly mixed aerosols in the environment remains challenging, because the laboratory mass spectral profile database of primary emissions is limited and the potential molecular specificity is impeded by intensive fragmentation in the AMS and ACSM.

To minimize the loss of the molecular information from fragmentation, soft ionization and novel sampling techniques have been deployed to measure the chemical composition of particles in greater detail. A thermal desorption aerosol gas chromatograph (TAG) coupled to a AMS has been used and provided the molecular characterization of OA and SOA (Bertrand et al., 2018). The filter inlet for gases and aerosols (FIGAERO) measures molecular composition of OA via thermal desorption coupled to a chemical-ionization mass spectrometer (Lopez-Hilfiker et al., 2014). Nonetheless, thermal decomposition can occur during the thermal desorption process (Stark et al., 2017), causing potential artifacts and hindering the identification of components. An extractive electrospray ionization time-of-flight mass spectrometer (EESI-TOF) has been recently developed for online OA measurement with generally insignificant decomposition or fragmentation (Lopez-Hilfiker et al.,

https://doi.org/10.5194/egusphere-2023-1102
Preprint. Discussion started: 30 May 2023

2019). As a result, it provides a molecular-level (i.e., molecular formula determination) mass spectrum with a time resolution of seconds. Consequently, improved real-time investigations of chemical composition in chamber experiments (Surdu et al., 2023; Bell et al., 2022) and SOA source apportionment in the field measurement (Tong et al., 2021; Kumar et al., 2022; Qi et al., 2022) became possible. Thus far, detailed study of primary emissions from complex sources, e.g. combustion, has not yet been conducted with the EESI-TOF, which necessitates the measurement to fully utilize the chemical resolution capabilities of EESI-TOF for characterizing mass spectra and supporting the source apportionment in the field.

In this work, we systematically characterize the POA composition using both AMS and EESI-TOF from a variety of burning fuels from both residential stoves (beech logs and a mixture of spruce and pine logs) and open combustion (spruce and pine branches and needles, straw, cow dung, and polyethylene plastic bags). The emission factors of trace gases are presented and possible molecular markers for the burning fuels in this study are discussed. This work allows for a better understanding of the POA chemical composition emitted from different burning sources and provides important reference spectra for source apportionment.

2 Materials and methods

2.1 Experimental setup and instrumentation

A total of 36 burning experiments were conducted using 6 different types of burning materials, including beech, spruce, pine, straw, cow dung, and plastic bags. Beech logs, spruce and pine logs, fresh spruce and pine branches and needles, as well as straw were sourced from a local forestry company in Würenlingen, Switzerland. Cow dung cakes (made of cow dung and straw) were collected from Goyla dairy, Delhi, India, and polyethylene plastic bags were bought in Delhi, India. To represent residential burning, logs of (1) beech and (2) spruce and pine were burned separately in a stove (Bruns et al., 2017). Agricultural waste combustion and forest fires were respectively represented by burning (1) straw and (2) a mixture of fresh branches and needles of spruce and pine in an open stainless steel cylinder (65 cm in diameter and 35 cm in height). Finally, the half-open stove (e.g. angithi) and waste burning in India and some other areas (Fleming et al., 2018), respectively, were represented by burning (1) cow dung cakes and (2) plastic bags on top of the stainless steel cylinder, with the fuel resting on a mesh steel plate. The experimental setup is shown in Figure S1. The fuels were ignited with fire starters / kindling and the emissions were pulled into either a chimney (for stove burning) or a hood (for open burning). After starters / kindling burnt away (~3 to 10 min. after ignition), the emissions were introduced into a stainless steel holding tank (1 m^3) through stainless steel sampling lines heated to 180 °C and passing through an ejection dilutor (DI-1000, Dekati Ltd.) with a dilution ratio of ~10. The emissions were injected into the holding tank for 10 to 30 min, depending on the emission source. Typically, the injection was stopped when the measured POA concentration was above ~20 µg/m^3 after ~60 times dilution in the sampling lines. In different burning experiments, POA concentrations in the holding tank varied between 1 to 5 mg m^{-3} prior to sampling line dilution. The holding tank was flushed overnight with clean air before each experiment, ensuring the background particle concentrations were less than 10 #/cm^3.

The emissions were delivered from the holding tank to sampling instruments via stainless steel lines (6 mm O.D.) for particles and via Teflon lines (6 mm O.D.) for gases. Gas analyzers were used for monitoring the concentration of CO (Horiba APMA-370), CO_2 (LI-COR LI-7000), and total hydrocarbon (THC) and methane (Horiba APHA-

https://doi.org/10.5194/egusphere-2023-1102
Preprint. Discussion started: 30 May 2023

370). Particle concentrations were measured using a scanning mobility particle sizer (SMPS, model 3938, TSI) scanning a range of 16 to 638 nm. An aethalometer (AE 33, Magee Scientific) was used to retrieve the concentration of equivalent BC (eBC). A long time-of-flight aerosol mass spectrometer (LTOF-AMS, Aerodyne Research, Inc.) was deployed for online, non-refractory particle characterization and a subset of experiments were performed with high-resolution time-of-flight AMS (HTOF-AMS, Aerodyne Research, Inc.). The aerosols sampled by both the SMPS and AMS were dried with a Nafion dryer (Perma Pure). The aerosol was continuously sampled by the AMS through a 100 μm critical orifice and focused by PM_1 aerodynamic lens. Mass spectra of positive ion fragments (*m/z* 10 to 400) were obtained with a TOF mass spectrometer and were analyzed with the software SQUIRREL (SeQUential Igor data RetRiEvaL) v.1.63 and PIKA (Peak Integration by Key Analysis) v.1.23 for the IGOR Pro software package (Wavemetrics, Inc.). A detailed description of AMS can be found in Decarlo et al. (2006).

EESI-TOF was deployed for a real-time and molecular-level (i.e., molecular formula) measurement of OA with minimal analyte fragmentation or decomposition (Lopez-Hilfiker et al., 2019). Before entering the EESI-TOF, the aerosol passes through an activated charcoal denuder to remove gas-phase species. The aerosol intersects a spray of charged droplets generated by an electrospray probe. Particles coagulate with the electrospray (ES) droplets, and water-soluble compounds are extracted into the solvent and then ionized via the Coulomb explosion mechanism as the droplets evaporate. 100 ppm sodium iodide (NaI) in pure water (MilliQ) was used as the electrospray solution, resulting in the formation of $[M + Na]^+$ (M is the analyte) adduct in the positive ionization mode. The EESI-TOF mass analyzer achieved a mass resolution of ~10000 at *m/z* 173 and 11000 at *m/z* 323. The EESI-TOF operated with a time resolution of 1 s, and alternated 1.5 min of background measurements (in which the sampled air passes through a high efficiency particulate air (HEPA) filter to remove particles) with 3.5 min of direct sampling. These data were pre-averaged to 5 s for further analysis. Ions are only considered as signals from emissions when their intensity difference between the particle measurement and the corresponding background measurement periods were 1.9 times bigger than the propagated standard errors over the measurement cycle. For those selected ions, their mass flux to the detector was calculated as Equation 1:

$$Mass_x = \frac{I_x \times MW_x \times 10^{18}}{N_a} \qquad \textit{Equation (1)}$$

where $Mass_x$ and I_x are respectively the mass flux (attograms per second, ag s^{-1}) and the ion flux of (counts per second, cps) of a group of detected ions with the same molecular weight. MW_x is the molecular weight of *x* (with the mass of the charge carrier, typically Na^+, removed) . N_a is Avogadro's number. To assist with the peak identification, filters were collected from emissions and were analyzed with an ultrahigh-resolution mass spectrometer (Orbitrap). The Orbitrap (Orbitrap Exploris 120, Thermo Fischer) has a mass resolving power of 140000 at *m/z* 200, and was operated in positive mode scanning from *m/z* 50 to 450.

2.2 Data analysis

The emission factor (EF) of species *i* was calculated using the carbon mass balance method (Radke and Ward, 1993), expressed in the unit of g kg^{-1}, as shown in Equation 2.

$$EF_i = \frac{m_i \cdot W_C}{\Delta CO + \Delta CO_2 + \Delta THC + \Delta OC + \Delta BC} \qquad \textit{Equation (2)}$$

https://doi.org/10.5194/egusphere-2023-1102
Preprint. Discussion started: 30 May 2023

where ΔCO, ΔCO_2, ΔTHC, ΔOC, and ΔBC are the background-corrected carbon mass concentrations of CO, CO_2, THC, OC (organic carbon), and BC. OC was calculated from the ratio of organic aerosol and the ratio of organic mass (OM) to OC (OM/OC) measured by AMS (Canagaratna et al., 2015). m_i is the mass concentration of species *i*. W_C is the carbon mass fraction of the burning fuel. The W_C was reported 0.46 for wood (Bertrand et al., 2017), 0.45 for straw (Li et al., 2007), 0.45 for cow dung (Font-Palma, 2019), and 0.84 for plastic bags (Li et al., 2001). In experiments, where BC is not available, the sum of OC and BC is considered equal to the particulate matter (PM) determined by SMPS. The effective density of particles applied in the SMPS is determined by comparing mass and volume distributions from the AMS and SMPS (Bahreini et al., 2005). As the contribution of particles to the total carbon is much smaller than the gases, these two methods have little differences calculating the denominator in Equation 2. Therefore, the EFs of CO, CO_2, and THC are consistent using both methods. However, it could be important for calculating the EFs for particulate species because of the possible discrepancy between the mass measured by the SMPS and AMS arising from, for example, the particle size and effective density. Additionally, the OM/OC acquired by the AMS also would add uncertainty when converting OM to OC because the high range of *m/z* without peak fitting is not included in OM/OC. More comparison is discussed in Sect. 3.1.

The combustion condition was characterized by the modified combustion efficiency (MCE, Equation 3) (Ward and Hardy, 1991). When the MCE is higher than 0.9, the combustion is considered as predominantly flaming. When the MCE is lower than 0.85, it is dominated by smoldering.

$$MCE = \frac{\Delta CO_2}{\Delta CO + \Delta CO_2} \qquad \textit{Equation (3)}$$

2.3 Identification of potential markers

The identification of potential markers for emissions was performed by Mann-Whitney U test (Mann and Whitney, 1947; Wilcoxon, 1945) which has been applied in many fields and for the current study has the advantage that it does not require a large volume of normally distributed samples (Rugiel et al., 2021; Tai et al., 2022). It tests the null hypothesis that the two population medians are equal against the alternative hypothesis that the two populations are not equal. When the *p*-value is smaller than the significance level of 0.1, the median of the tested sample is significantly high or low in the two-tailed test. Ions from a class of fuel that satisfy the pairwise comparison test between one fuel *j* and other types of fuels were considered to be significantly high-fraction or low-fraction ions in the fuel *j* and therefore have the potential as markers for the fuel *j*. The fold change (FC) of ion *i* in the fuel *j* was calculated as the Equation 4, where the $f_{i,j}$ is the fraction of ion *i* in the mass spectra profiles of the fuel *j*, and $f_{i,other}$ is the average fraction of ion *i* in the mass spectra from the other fuels.

$$FC_{i,j} = \frac{f_{i,j}}{f_{i,other}} \qquad \textit{Equation (4)}$$

3 Results and discussion

3.1 Emission factors from combustion

The average EFs of CO, CO_2, THC, PM, OM, and eBC as well as the MCE values of the 6 types of burning are shown in Table 1, and the EFs and MCE values for each experiment are presented in Table S1.

https://doi.org/10.5194/egusphere-2023-1102
Preprint. Discussion started: 30 May 2023

The average MCE values depend on fuel types, with the lowest values of 0.87 ± 0.03 (average ± 1 σ) observed from cow dung open burning and the highest values of 0.98 ± 0.02 from plastic bags open burning, consistent with smoldering combustion for cow dung and flaming/melting processes for plastic bags. Accordingly, cow dung had the highest average CO EF (92.3 ± 27.4 g kg^{-1}) and the lowest CO_2 EF (1366.2 ± 88.4 g kg^{-1}), and vice versa for plastic bags. The strong relationship between the MCE and some EFs is also true for the THC. In general, lower the MCEs correspond to higher THC EFs within a given class of burning fuel. Taking straw burning as an example, the EFs of THC vary from 0.7 to 39.3 g kg^{-1}, with the MCE varying from nearly 1.00 to 0.89 correspondingly. These EFs of gases are comparable with the reported EFs from the literatures under similar conditions (Hennigan et al., 2011; Fang et al., 2017; Bertrand et al., 2017).

The average EFs of PM is in the range of 3.1 to 16.6 g kg^{-1}. In general, the PM emitted from cow dung is dominated by OM, and the eBC is minor. For beech logs and straw, the OM EF is around 3 times higher than the eBC EF. Noticeably, the emission of PM from plastic bags is not very high (3.0 g kg^{-1}), but the EF of OM and eBC is similar (1.5 g kg^{-1} v.s. 1.0 g kg^{-1}). Note that when eBC data is not available, the sum of OC and BC in the denominator in Equation 2 is assumed to be equal to the PM measured by the SMPS. Table S1 lists the comparison of EFs for particulate species where possible. For the experiments of cow dung open burning and plastic bags open burning, the EFs are consistent using both methods with the difference of PM EF < 6%, and on average less than 15% for OM EF. However, for some beech logs stove burning experiments (BS3 and BS4), the effective density required in the calculation is not available, and the average density of other beech logs in this study is used. This results in some variance between these two methods.

3.2 Chemical composition of POAs from combustion

3.2.1 Chemical composition of POAs measured with the AMS

The chemical composition of POAs of burning emissions are characterized with the AMS and EESI-TOF simultaneously. As shown in Figure 1, the average mass spectra from *m/z* 10 to 120 measured with AMS is grouped into C_xH_y, $C_xH_yO_1$, $C_xH_yO_{2+}$, and $C_xH_yN_z$ families based on their elemental composition. The mass spectrum of plastic bags burning is not shown because considerable $C_xH_yO_z$ family was observed (23%), but it is more likely from the emission remaining in the tubing of other fuels than from the plastic bags given the fact that polyethylene is the main component of it. In all the POAs, the C_xH_y-family is the most abundant group, mainly from ions at m/z 29, 39, 41, 43, 55, 57, 67, and 69 originating primarily from hydrocarbon compounds, with the biggest contribution for cow dung (72%) and straw (62%), generally higher than that of wood (beech, spruce, and pine, 48% to 55%) burning. The $C_xH_yO_{2+}$ and $C_xH_yO_1$ families are the second largest compositions, with major ions at *m/z* 28, 29, 43, 44, and 60, which are higher in wood and straw emissions compared to cow dung. Among these ions, the mass fractions of *m/z* 44 (f_{44}, mostly CO_2^+), *m/z* 43 (f_{43}, mostly $C_2H_3O^+$ and $C_3H_7^+$), and *m/z* 60 (f_{60}, mostly $C_2H_4O_2^+$) have the largest impact on the oxidation state of the aerosol. The fragment $C_2H_4O_2^+$ at *m/z* 60 is widely used as a levoglucosan related marker for biomass burning and is most prominent in the wood burning emissions compared to the other burning fuels. Figure 2a shows that the POAs in this study are at the left bottom of the ambient OOA range (Ng et al., 2010) in the f_{44} vs f_{43} plot, indicating the POA is less oxygenated, which is consistent with previous studies (Hennigan et al., 2011; Fang et al., 2017; Xu et al., 2020). As shown in Figure 2b, the f_{60} for the biomass source studied is greater than the background level (Cubison et al., 2011), suggesting the f_{60} filter in the ambient is unlikely to miss biomass combustion. The contribution of f_{60} relates to the burning

https://doi.org/10.5194/egusphere-2023-1102
Preprint. Discussion started: 30 May 2023

fuel types and the combustion efficiency. For example, the f_{60} from wood burning ranges from 0.02 to 0.04, generally higher than that of cow dung. The f_{60} of straw open burning is distributed from below 0.01 to 0.025, resulting from the low to high MCE values correspondingly. The pie charts in Figure 1 indicate that the N-containing fragments from AMS are mainly from $C_xH_yN_z$ family and it is the largest in the emission of cow dung open burning (~3%) and followed by straw (~2%), while the wood is relatively minimal (≤ 1%) (Stockwell et al., 2016). The nitrogen in organonitrates would appear mainly at fragments of NO^+ and NO_2^+. However, the NO^+ and NO_2^+ originating from organonitrates are estimated almost 20 times smaller than $C_xH_yN_z$ family in cow dung burning using the NO^+ and NO_2^+ ratio between inorganic nitrates and organonitrates (Farmer et al., 2010), suggesting their contributions are minor to organic nitrogen.

In the region from *m/z* 120 to 450 as shown in Figure S2, polycyclic aromatic hydrocarbons (PAHs) are observed. Based on the spectra of laboratory standards (Dzepina et al., 2007; Aiken et al., 2007), parent ions at *m/z* 239, 252, 276, 300, and 326 correspond respectively to $C_{19}H_{12}$ (methylbenzofluoranthene), $C_{20}H_{12}$ (benzofluoranthene and benzopyrene), $C_{22}H_{12}$ (indenopyrene and benzoperylene), $C_{24}H_{12}$ (coronene), and $C_{26}H_{14}$ (dibenzoperylene). These ions contribute 0.69% ± 0.14% and 0.66% ± 0.11% respectively to the total POA of the spruce and pine branches and needles open burning as well as spruce and pine logs stove burning, which is distinct from straw (0.36% ± 0.13%), beech logs (0.34% ± 0.14%), and cow dung (0.25% ± 0.13%). The lower bound of the contribution of these ions for plastic bags is estimated as 0.57% ± 0.37%. Of particular note is the series of high intensity ions at *m/z* >350 in emissions from the plastic bags open burning. Reference mass spectra of PAHs at higher mass-to-charge ratio (> *m/z* 350) is not available so far, but from the PAH pattern of spikes spacing ~24 – 26 amu, we speculate that this series does come from a series of high molecular weight PAHs.

3.2.2 Chemical composition of POAs measured with the EESI-TOF

The EESI-TOF provides an important complement to the highly fragmented mass spectra generated by the AMS, where intact compounds measured by the EESI-TOF from *m/z* 100 to 400 are shown in Figure 3. The bin of compounds containing O/C greater than 0.7 has the largest and similar contribution in wood burning (29.9% to 31.5%), and it is slightly smaller in straw (25%) and cow dung (20.1%). O/C smaller than 0.15 contributes 15.3% to 18.8% in spruce and pine which is similar to the fraction in cow dung (13.5%) but much higher compared to beech logs (4.7%) and straw (8.8%), mainly due to the greater contribution of compounds with carbon numbers in the range of 18 to 21. Cow dung has a slightly lower fraction of low-H/C and a slightly higher fraction of high-H/C comparing to other fuels studied.

As shown in the pie charts in Figure 3, the $C_xH_yO_z$-family is the main group measured by the EESI-TOF with contribution from 80% to 97%. The N-containing species have the highest contribution (19.6%) in the POA from cow dung open burning, which is much higher than other fuels in this study (2.5% to 8.9%). Of the N-containing species in cow dung POA 95% contain one nitrogen atom and are in a wide range of carbon number between 5 and 22, with mainly in the O/C range of < 0.15 to 0.5 and the H/C from 1.2 to > 1.7 (Figure S3). The degree of unsaturation, calculated from the ratio of the double-bond equivalent to the number of carbons (DBE/C). The difference in all the studied POAs is not major (Figure S4).

On molecular level, $C_6H_{10}O_5$ (*m/z* 162.0523) is most abundant in wood combustion (20.3% ± 6.1%), is less pronounced in straw (15.0%% ± 7.9%) and even less so in cow dung emissions (9.9% ± 5.4%) (Figure 2c). It could be mainly assigned to levoglucosan (or similar dehydrated sugars) which is formed from the pyrolysis of

https://doi.org/10.5194/egusphere-2023-1102
Preprint. Discussion started: 30 May 2023

cellulose and hemicellulose (Simoneit, 2002). The second most abundant species presented in the POAs is $C_8H_{12}O_6$ (*m/z* 204.0628) in this study, contributing between 2 and 9%. It has been observed from the primary biomass burning emissions in the laboratory and ambient studies (Kumar et al., 2022; Kong et al., 2021). In addition, compounds with 18 and 20 carbon atoms are rich in many fuel types, particularly in spruce and pine burning emissions, and are notably minimal in beech logs.

The O/C (calculated as the ratio of total oxygen to total carbon) of the POAs from 5 types of burning measured by the EESI-TOF is 0.32 – 0.41, which is higher than that of the AMS (0.16 – 0.37). The difference likely occurs because the EESI-TOF is insensitive to species with low water solubility and/or low affinity for Na^+ (e.g., hydrocarbons including polyaromatic hydrocarbons). This may also contribute to an underestimation of H/C. The total nitrogen-to-total carbon ratio (N/C) of cow dung measured by EESI-TOF is 0.019, which is slightly higher than that in the AMS measurements (0.015). This could be partially because of the difference in EESI sensitivity to the N-containing molecules. Another reason is that the total carbon from OA measured by the EESI-TOF is smaller, again consistent with the absence of non-water-soluble substances or molecules that do not bind to Na^+.

3.3 Common markers for solid-fuel combustion

Levoglucosan and dehydrated sugars having the molecular formula $C_6H_{10}O_5$ are commonly used as tracers for biomass burning. A range of values for the fraction of $C_6H_{10}O_5$ is observed both for the same fuel type under different burning conditions and for different fuel types, as seen in Figure 2c. Thus, $C_6H_{10}O_5$ is a good untargeted marker for biomass burning, but cannot be used to determine the specific source (or type of combustible) responsible for biomass burning emissions. Likewise, the $C_8H_{12}O_6$ is not a suitable marker for specific emission sources, as it is prevalent in all burns of biomass material. Additionally, $C_8H_{12}O_6$ has been considered as a tracer for terpene or syringol-derived SOA (Szmigielski et al., 2007; Yee et al., 2013), however our results suggest this molecular formula is not a good marker for SOAs due to the strong contribution from biomass burning-derived POA.

At a higher mass range, $C_{16}H_{32}O_2$ and $C_{18}H_{30,32,34}O_2$ are likely to be the common saturated and unsaturated fatty acids corresponding to palmitic, linolenic, linoleic, and oleic acid, which are important structural components of cells and were found in the emission of cooking, biomass burning, and cow dung (Simoneit, 2002; Neves et al., 2009a; Neves et al., 2009b; Brown et al., 2021). The corresponding compounds for the $C_{20}H_{30}O_2$ are most likely resin acids (e.g., abietic acid and pimaric acid) which have been specifically found in coniferous wood species (Holmbom, 1977) and served as biomass burning tracers (Simoneit et al., 1993; Liang et al., 2021). The $C_{20}H_{30,32,24}O_{2,3}$ have been found as diterpenoids from the wood of Cunninghamia konishii (Li and Kuo, 2002). This plant species belongs to the class of Pinopsida, which also includes spruce and pine.

These typical markers stated above are well-known, but due to their presence in more than one fuel, the determination of different BB sources (or even biomass burning-derived POA) is challenging. For example, scaling levoglucosan to total BB OM requires a priori knowledge of the BB source and burning condition (Favez et al., 2010). Therefore, it is complicated to apply these markers in the source apportionment without comparison to statistically rule out other possibilities.

https://doi.org/10.5194/egusphere-2023-1102
Preprint. Discussion started: 30 May 2023

3.4 Identification of potential markers for specific solid fuels

To investigate the feasibility of distinguishing differences between the combustion fuel sources based on the measured species, the similarity of mass spectra acquired from each experiment by AMS and EESI-TOF is assessed with Spearman's rank correlation coefficient (r), as shown in Figure 4. In the correlation matrix with the fragment ions from AMS (Figure 4a), it is clear that the POAs from the same burning fuel strongly correlate. For instance, the average correlation coefficients of the AMS POA MS for all experiments using the same fuel range from 0.84 to 0.95. When comparing different fuels, a strong correlation is also found between spruce and pine logs stove burning and spruce and pine branches and needles open burning (0.95 ± 0.02). This is mainly because these two types of burning are closely related (i.e., derived from the same plants), and therefore have similar chemical composition. The correlation weakened when comparing POAs from different materials (e.g., spruce – beech 0.77 ± 0.03, spruce – straw 0.76 ± 0.03, spruce – cow dung 0.75 ± 0.03).

By contrast, the correlation coefficients based on the species from EESI-TOF are much lower among different burning fuels and even amongst the same fuel type (0.44 to 0.68). Noticeably, only a weak intra-fuel correlation is found for spruce/pine logs stove burning (0.44 ± 0.07), indicating that there are significant differences between experiments which are likely driven by burn-to-burn variability caused by differences in the combustion condition or variance of the fuel materials (e.g., with or without bark, amount of sap in the wood, etc.). Nevertheless, the variability between different fuels is clearly larger than the intra-fuel variability for the POAs. For example, the correlation between the cow dung and all the other fuels (average 0.27 ± 0.11) is significantly lower than that of among cow dung emissions (0.49 ± 0.16). This suggests that the EESI-TOF may be capable of distinguishing between different types of BB fuels.

To perform a more detailed analysis and identify markers between the emissions, the Mann-Whitney U test (see Sect. 2.2) of the POAs from different fuels measured by AMS and EESI-TOF is conducted. Considering that both spruce and pine logs stove burning as well as spruce and pine branches and needles are similar fuel types and have a comparable POA composition in Figures 1 to 3, they were classified as the same fuel for this test. Results of the Mann-Whitney U test are presented in Figure 5, where we show the average $-\log_{10}$ of the p-value as a function of the $\log_2$ of the fold change (FC). Species having p-values less than 0.1 in the two-tailed test in all pairwise comparisons are considered to be significantly more prevalent or scarcer in a single fuel compared to all other fuels. These ions are represented as colored circles in Figure 5. If the species fail to meet the criterion one time or more than one time, those species will be shown as gray circles even though their average p-value might be lower than 0.1. A higher $-\log_{10}(p\text{-value})$ (i.e., a lower p-value) indicates a lower probability that the fractional medians of two species are equal. At the same time, a higher FC (Equation 4) indicates a higher abundance of the species' fractional contribution in the tested fuel compared to the average of all other fuels, deeming it more exclusive. In the case of beech logs as well as spruce and pine logs burning, the colored p-value is lower (higher $-\log_{10}(p\text{-value})$) in the dataset of AMS than that of EESI-TOF, suggesting the results from the AMS are more replicable. However, from the perspective of FC, its absolute value is around 2 to 4 times higher in the dataset of the EESI-TOF than that of the AMS. This shows that the potential markers selected from the EESI-TOF measurement are more unique, in some cases found only in the spectrum of a given source. On this ground, the AMS and EESI-TOF are potent complementary tools to provide separation and source apportionment of ambient OA, and to capture marker compounds. The selected potential markers, p-values, and fold changes are listed in Table S2 and Table S3 for EESI-TOF and AMS data, respectively.

https://doi.org/10.5194/egusphere-2023-1102
Preprint. Discussion started: 30 May 2023

Mass defect plots of the selected marker compounds are visualized in Figure 6. Many more potential markers are identified from spruce and pine burning, as well as cow dung open burning, in comparison to beech and straw burning. As shown in Figure 6A with the AMS dataset, potential markers from C_xH_y and $C_xH_yO_z$-family have significantly higher fraction in the POA of beech logs than those in other fuels. By contrast, the selected markers for spruce and pine burning are more oxidized and mainly composed of $C_xH_yO_z$-family, which is consistent with its bulk chemical composition and relatively higher O/C. The main fragments CO^+ and CO_2^+ have higher contributions in spruce and pine burning (also can be seen in Figure 1), but their FCs are not very high, which means they are not exclusive in spruce and pine and therefore are not applicable as sole tracers in the complex ambient air. Fragments from cow dung open burning have considerably higher contribution in C_xH_y -family and N-containing families, but lower in oxygen-containing species, which also agrees with bulk chemical composition characteristics.

Similarly, many marker compounds are determined in the measurement of EESI-TOF for spruce and pine burning as well as cow dung open burning. Compounds with $20 - 21$ carbon atoms as shown in Figure 6B for spruce and pine burning could be resin and conifer needle-related, such as $C_{20}H_{32}O_3$ (likely isocupressic acid) (Mofikoya et al., 2020; Wiyono et al., 2006). Homologues of $C_{11}H_{12}(CH_2)_{0\text{-}3}O_7$ are also determined, of which $C_{14}H_{18}O_7$ could be picein which is an important phenolic compound in the needles of spruce (Løkke, 1990). On the other hand, some compounds which are barely present in the POA of spruce and pine burning, such as $C_{14}H_{28}(CH_2)_{0\text{-}3}O_2$ (likely saturated fatty acids), offers an alternative perspective of exclusion method in source separation. Noticeably, while coniferyl alcohol ($C_{10}H_{12}O_3$) is a major pyrolysis product from softwood (e.g., spruce) lignins (Saiz-Jimenez and De Leeuw, 1986) and has a decent fractional contribution in POA of the spruce and pine burning, but its contribution in spruce and pine burning is smaller than straw burning. Therefore, it is not recommended as a tracer when other biomass fuels are present. For the hardwood (i.e., beech logs in this study), sinapyl alcohol ($C_{11}H_{14}O_4$) is one of the prominent products from pyrolysis of lignins (Saiz-Jimenez and De Leeuw, 1986) and is conspicuous in our beech logs stove burning. Interestingly, nitrogen-containing compound $C_{13}H_{17}NO_6$ is noted as a tracer for straw open burning, and the nitrogen-containing fragments $C_3H_{8\text{-}9}N$ are also selected from the straw AMS analysis.

Cow dung is a clearly different fuel to other biomass fuels in this study, thus many markers are identified from cow dung open burning. These potential markers have mostly nitrogen in chemical composition and with generally higher FC. Many series of N-containing homologues are found, such as $C_{10}H_9NO_2$ and $C_{11}H_{11}NO_2$, which could be likely assigned to the derivative of indole, i.e., indole acetic acid and indolepropionic acid respectively. Another series of homologues is $C_9H_{11}NO_2$ and $C_{10}H_{13}NO_2$, which have been found especially in the emissions from cow dung cook fire in India compared to brushwood cook fire (Fleming et al., 2018). Homologues without nitrogen atoms in the chemical composition are also seen, for example, $C_{22}H_{42}(CH_2)_{0\text{-}2}O_2$, likely the homologues of erucic acid which is a natural fatty oil mainly present in the Brassicaceae family of plants. Nevertheless, it is not very surprising to see the biomass-related species as cows are herbivorous animals.

To the best of our knowledge, most of these markers are reported for the first time in POA emissions from the studied fuels. They could improve the refinement in source separation of fuels in biomass burning. Replicability and specificity are two important criteria for tracers. The *p*-value being less than 0.1 in the two-tailed test can ensure the stability of the shown results. The FC tells the degree of specificity of markers of one fuel in the presence of other fuels. If the *p*-value criterion is satisfied and the FC is large, the presence of this marker can

https://doi.org/10.5194/egusphere-2023-1102
Preprint. Discussion started: 30 May 2023

directly lead us to the emission source. On the other hand, if the FC is less than 1, the detection of this compound can decisively exclude the related source after verifying this isn't due to a detection limit issue. However, if the FC is in-between, more caution is needed because these compounds don't have a distinctive fraction in that fuel compared to other fuels, but could have a relatively fixed ratio compared to other markers.

4 Conclusions

In this study, we conducted 36 burning experiments to simulate typical solid fuel combustion emission, including residential burning (beech or spruce and pine logs stove burning), wildfire (spruce and pine braches and needles open burning), agricultural residue in field burning (straw open burning), cow dung open burning, and plastic bags open burning. The emission factors of CO, CO_2, THC, PM, OM, and BC were determined. The chemical composition of particles emitted from the combustion processes was comprehensively characterized using the AMS and the EESI-TOF, and the chemical composition of the particles measured by the two instruments were compared. These are the first direct measurements of these source profiles with the EESI-TOF. The utility of traditional markers are discussed, and new potential markers were identified using the Mann-Whitney U test.

The EFs of CO and THC are generally higher during the low combustion efficiency, and the opposite for the EF of CO_2. The highest EF of PM (16.6±10.8 g kg^{-1}) is from cow dung open burning which is mostly OM (16.2±10.8 g kg^{-1}), but for residential and plastic bags burning, the eBC accounts for ~30% of the total PM. The organics measured by the AMS show that the wood (beech, spruce, and pine) burning emission has a relatively higher abundance of $C_xH_yO_z$ fragments, while straw and cow dung burning emissions are dominated by C_xH_y fragments in their POAs. On the molecular level, $C_6H_{10}O_5$ has the highest proportion (~7% to ~30%) in the POAs measured by the EESI-TOF (except for the plastic bags burning), followed by $C_8H_{12}O_6$ with fractions of ~2% to ~9%. The chemical composition measured with AMS covers a wide range of non-refractory organic and inorganic components. However, the extensive fragmentation concentrates the measured mass-to-charge ratio below ~120 and limits its chemical resolution. The chemical groups used to deduce the composition of particles could originate from different compounds, which impedes us from seeing the full picture. The formula-based mass spectrum from the EESI-TOF overcomes this deficiency and thus reveals the detailed characteristics.

However, many compounds are present ubiquitously in all of the fuels used here, making it challenging to identify atmospheric sources solely by visual comparisons of the full mass spectra. By using the Mann-Whitney U test to identify potential markers among the studied fuels, we find that the markers identified by the AMS have greater replicability and by EESI-TOF are more distinctive, thus providing an important reference for the source apportionment. Markers identified with the EESI-TOF from spruce and pine burning with $20-21$ carbon atoms could be resin and conifer needle-related. The product from pyrolysis of hardwood lignins is found specially in beech logs stove burning. Nitrogen-containing homologues are identified particularly from cow dung open burning. Overall, this work highlights the characteristics of POAs emitted from the burning of solid fuels and proposes the markers for separating different sources using the AMS and EESI-TOF.

In the future, the volatility and chemical reactivity of the proposed markers should be tested to determine their atmospheric stability and their ability to be a robust marker. More burning fuels such as coal and grass could be conducted to enrich the spectral database.

https://doi.org/10.5194/egusphere-2023-1102
Preprint. Discussion started: 30 May 2023

Data availability

The datasets are available upon request to the corresponding authors.

Author contributions

JZ, TTW, KL, DMB, EG, KYC, and SB conducted the burning experiments. JZ analyzed the data and wrote the manuscript. DSW, MS, TQC, LQ, and DB participated in the campaign. DMB, KL, IEH, HL, JGS, and ASHP participated in the interpretation of data.

Competing interests

The authors declare that they have no conflict of interest.

Disclaimer

Publisher's note: Copernicus Publications remains neutral with regard to jurisdictional claims in published maps and institutional affiliations.

Acknowledgements

This work was supported by the Swiss National Science Foundation (SNSF) SNF grant MOLORG (200020_188624), the European Union's Horizon 2020 research and innovation programme through the ATMO-ACCESS Integrating Activity under grant agreement no. 101008004, and the European Union's Horizon 2020 research and innovation programme under the Marie Skłodowska-Curie grant agreement No 884104 (PSI-FELLOW-III-3i).

Reference

Adam, M. G., Tran, P. T. M., Bolan, N., and Balasubramanian, R.: Biomass burning-derived airborne particulate matter in Southeast Asia: A critical review, J Hazard Mater, 407, 124760, https://www.ncbi.nlm.nih.gov/pubmed/33341572, 2021.

Aiken, A. C., DeCarlo, P. F., and Jimenez, J. L.: Elemental Analysis of Organic Species with Electron Ionization High-Resolution Mass Spectrometry, Anal. Chem., 79, 8350-8358, https://doi.org/10.1021/ac071150w, 2007.

Alfarra, M. R., Prevot, A. S. H., Szidat, S., Sandradewi, J., Weimer, S., Lanz, V. A., Schreiber, D., Mohr, M., and Baltensperger, U.: Identification of the Mass Spectral Signature of Organic Aerosols from Wood Burning Emissions, Environmental Science & Technology, 41, 5770-5777, https://doi.org/10.1021/es062289b, 2007.

Andreae, M. O.: Emission of trace gases and aerosols from biomass burning – an updated assessment, Atmos. Chem. Phys., 19, 8523-8546, https://acp.copernicus.org/articles/19/8523/2019/, 2019.

Bahreini, R., Keywood, M. D., Ng, N. L., Varutbangkul, V., Gao, S., Flagan, R. C., Seinfeld, J. H., Worsnop, D. R., and Jimenez, J. L.: Measurements of Secondary Organic Aerosol from Oxidation of Cycloalkenes, Terpenes, and m-Xylene Using an Aerodyne Aerosol Mass Spectrometer, Environ. Sci. Technol., 39, 5674-5688, https://doi.org/10.1021/es048061a, 2005.

Bell, D. M., Wu, C., Bertrand, A., Graham, E., Schoonbaert, J., Giannoukos, S., Baltensperger, U., Prevot, A. S. H., Riipinen, I., El Haddad, I., and Mohr, C.: Particle-phase processing of α-pinene NO3 secondary organic aerosol in the dark, Atmos. Chem. Phys., 22, 13167-13182, https://acp.copernicus.org/articles/22/13167/2022/, 2022.

Bertrand, A., Stefenelli, G., Bruns, E. A., Pieber, S. M., Temime-Roussel, B., Slowik, J. G., Prévôt, A. S. H., Wortham, H., El Haddad, I., and Marchand, N.: Primary emissions and secondary aerosol production potential

https://doi.org/10.5194/egusphere-2023-1102
Preprint. Discussion started: 30 May 2023

from woodstoves for residential heating: Influence of the stove technology and combustion efficiency, Atmos. Environ., 169, 65-79, https://www.sciencedirect.com/science/article/pii/S1352231017305861, 2017.
Bertrand, A., Stefenelli, G., Jen, C. N., Pieber, S. M., Bruns, E. A., Ni, H., Temime-Roussel, B., Slowik, J. G., Goldstein, A. H., El Haddad, I., Baltensperger, U., Prévôt, A. S. H., Wortham, H., and Marchand, N.: Evolution of the chemical fingerprint of biomass burning organic aerosol during aging, Atmos. Chem. Phys., 18, 7607-7624, https://acp.copernicus.org/articles/18/7607/2018/, 2018.
Bond, T. C., Bhardwaj, E., Dong, R., Jogani, R., Jung, S., Roden, C., Streets, D. G., and Trautmann, N. M.: Historical emissions of black and organic carbon aerosol from energy-related combustion, 1850–2000, Global Biogeochem. Cycles, 21, https://agupubs.onlinelibrary.wiley.com/doi/abs/10.1029/2006GB002840, 2007.
Brown, W. L., Day, D. A., Stark, H., Pagonis, D., Krechmer, J. E., Liu, X., Price, D. J., Katz, E. F., DeCarlo, P. F., Masoud, C. G., Wang, D. S., Hildebrandt Ruiz, L., Arata, C., Lunderberg, D. M., Goldstein, A. H., Farmer, D. K., Vance, M. E., and Jimenez, J. L.: Real-time organic aerosol chemical speciation in the indoor environment using extractive electrospray ionization mass spectrometry, Indoor Air, 31, 141-155, https://www.ncbi.nlm.nih.gov/pubmed/32696534, 2021.
Bruns, E. A., Slowik, J. G., El Haddad, I., Kilic, D., Klein, F., Dommen, J., Temime-Roussel, B., Marchand, N., Baltensperger, U., and Prévôt, A. S. H.: Characterization of gas-phase organics using proton transfer reaction time-of-flight mass spectrometry: fresh and aged residential wood combustion emissions, Atmos. Chem. Phys., 17, 705-720, https://acp.copernicus.org/articles/17/705/2017/, 2017.
Canagaratna, M. R., Jimenez, J. L., Kroll, J. H., Chen, Q., Kessler, S. H., Massoli, P., Hildebrandt Ruiz, L., Fortner, E., Williams, L. R., Wilson, K. R., Surratt, J. D., Donahue, N. M., Jayne, J. T., and Worsnop, D. R.: Elemental ratio measurements of organic compounds using aerosol mass spectrometry: characterization, improved calibration, and implications, Atmos. Chem. Phys., 15, 253-272, https://acp.copernicus.org/articles/15/253/2015/, 2015.
Census of India: Households by Availability of Separate Kitchen and Type of Fuel Used for Cooking, available at: https://censusindia.gov.in/census.website/data/census-tables, 2011.
Chen, G., Sosedova, Y., Canonaco, F., Fröhlich, R., Tobler, A., Vlachou, A., Daellenbach, K. R., Bozzetti, C., Hueglin, C., Graf, P., Baltensperger, U., Slowik, J. G., El Haddad, I., and Prévôt, A. S. H.: Time-dependent source apportionment of submicron organic aerosol for a rural site in an alpine valley using a rolling positive matrix factorisation (PMF) window, Atmos. Chem. Phys., 21, 15081-15101, https://acp.copernicus.org/articles/21/15081/2021/, 2021.
Chen, J., Li, C., Ristovski, Z., Milic, A., Gu, Y., Islam, M. S., Wang, S., Hao, J., Zhang, H., He, C., Guo, H., Fu, H., Miljevic, B., Morawska, L., Thai, P., Lam, Y. F., Pereira, G., Ding, A., Huang, X., and Dumka, U. C.: A review of biomass burning: Emissions and impacts on air quality, health and climate in China, Sci. Total Environ., 579, 1000-1034, https://www.sciencedirect.com/science/article/pii/S0048969716324561, 2017.
Crippa, M., Canonaco, F., Lanz, V. A., Äijälä, M., Allan, J. D., Carbone, S., Capes, G., Ceburnis, D., Dall'Osto, M., Day, D. A., DeCarlo, P. F., Ehn, M., Eriksson, A., Freney, E., Hildebrandt Ruiz, L., Hillamo, R., Jimenez, J. L., Junninen, H., Kiendler-Scharr, A., Kortelainen, A. M., Kulmala, M., Laaksonen, A., Mensah, A. A., Mohr, C., Nemitz, E., O'Dowd, C., Ovadnevaite, J., Pandis, S. N., Petäjä, T., Poulain, L., Saarikoski, S., Sellegri, K., Swietlicki, E., Tiitta, P., Worsnop, D. R., Baltensperger, U., and Prévôt, A. S. H.: Organic aerosol components derived from 25 AMS data sets across Europe using a consistent ME-2 based source apportionment approach, Atmos. Chem. Phys., 14, 6159-6176, https://acp.copernicus.org/articles/14/6159/2014/, 2014.
Cubison, M. J., Ortega, A. M., Hayes, P. L., Farmer, D. K., Day, D., Lechner, M. J., Brune, W. H., Apel, E., Diskin, G. S., Fisher, J. A., Fuelberg, H. E., Hecobian, A., Knapp, D. J., Mikoviny, T., Riemer, D., Sachse, G. W., Sessions, W., Weber, R. J., Weinheimer, A. J., Wisthaler, A., and Jimenez, J. L.: Effects of aging on organic aerosol from open biomass burning smoke in aircraft and laboratory studies, Atmos. Chem. Phys., 11, 12049-12064, https://acp.copernicus.org/articles/11/12049/2011/, 2011.
Daellenbach, K. R., Uzu, G., Jiang, J., Cassagnes, L.-E., Leni, Z., Vlachou, A., Stefenelli, G., Canonaco, F., Weber, S., Segers, A., Kuenen, J. J. P., Schaap, M., Favez, O., Albinet, A., Aksoyoglu, S., Dommen, J., Baltensperger, U., Geiser, M., El Haddad, I., Jaffrezo, J.-L., and Prévôt, A. S. H.: Sources of particulate-matter air pollution and its oxidative potential in Europe, Nature, 587, 414-419, https://doi.org/10.1038/s41586-020-2902-8, 2020.
de Oliveira Alves, N., Vessoni, A. T., Quinet, A., Fortunato, R. S., Kajitani, G. S., Peixoto, M. S., Hacon, S. d. S., Artaxo, P., Saldiva, P., Menck, C. F. M., and Batistuzzo de Medeiros, S. R.: Biomass burning in the Amazon region causes DNA damage and cell death in human lung cells, Sci. Rep., 7, 10937, https://doi.org/10.1038/s41598-017-11024-3, 2017.
DeCarlo, P. F., Kimmel, J. R., Trimborn, A., Northway, M. J., Jayne, J. T., Aiken, A. C., Gonin, M., Fuhrer, K., Horvath, T., Docherty, K. S., Worsnop, D. R., and Jimenez, J. L.: Field-Deployable, High-Resolution, Time-of-Flight Aerosol Mass Spectrometer, Anal. Chem., 78, 8281-8289, https://doi.org/10.1021/ac061249n, 2006.
Dzepina, K., Arey, J., Marr, L. C., Worsnop, D. R., Salcedo, D., Zhang, Q., Onasch, T. B., Molina, L. T., Molina, M. J., and Jimenez, J. L.: Detection of particle-phase polycyclic aromatic hydrocarbons in Mexico City using an

https://doi.org/10.5194/egusphere-2023-1102
Preprint. Discussion started: 30 May 2023

aerosol mass spectrometer, Int. J. Mass Spectrom., 263, 152-170, https://doi.org/10.1016/j.ijms.2007.01.010, 2007.
Fang, Z., Deng, W., Zhang, Y., Ding, X., Tang, M., Liu, T., Hu, Q., Zhu, M., Wang, Z., Yang, W., Huang, Z., Song, W., Bi, X., Chen, J., Sun, Y., George, C., and Wang, X.: Open burning of rice, corn and wheat straws: primary emissions, photochemical aging, and secondary organic aerosol formation, Atmos. Chem. Phys., 17, 14821-14839, https://doi.org/10.5194/acp-17-14821-2017, 2017.
Farmer, D. K., Matsunaga, A., Docherty, K. S., Surratt, J. D., Seinfeld, J. H., Ziemann, P. J., and Jimenez, J. L.: Response of an aerosol mass spectrometer to organonitrates and organosulfates and implications for atmospheric chemistry, Proc Natl Acad Sci U S A, 107, 6670-6675, https://www.ncbi.nlm.nih.gov/pubmed/20194777, 2010.
Favez, O., El Haddad, I., Piot, C., Boréave, A., Abidi, E., Marchand, N., Jaffrezo, J. L., Besombes, J. L., Personnaz, M. B., Sciare, J., Wortham, H., George, C., and D'Anna, B.: Inter-comparison of source apportionment models for the estimation of wood burning aerosols during wintertime in an Alpine city (Grenoble, France), Atmos. Chem. Phys., 10, 5295-5314, https://acp.copernicus.org/articles/10/5295/2010/, 2010.
Fleming, L. T., Lin, P., Laskin, A., Laskin, J., Weltman, R., Edwards, R. D., Arora, N. K., Yadav, A., Meinardi, S., Blake, D. R., Pillarisetti, A., Smith, K. R., and Nizkorodov, S. A.: Molecular composition of particulate matter emissions from dung and brushwood burning household cookstoves in Haryana, India, Atmos. Chem. Phys., 18, 2461-2480, https://acp.copernicus.org/articles/18/2461/2018/, 2018.
Font-Palma, C.: Methods for the Treatment of Cattle Manure—A Review, C, 5, http://doi.org/10.3390/c5020027, 2019.
Hennigan, C. J., Miracolo, M. A., Engelhart, G. J., May, A. A., Presto, A. A., Lee, T., Sullivan, A. P., McMeeking, G. R., Coe, H., Wold, C. E., Hao, W. M., Gilman, J. B., Kuster, W. C., de Gouw, J., Schichtel, B. A., Collett, J. L., Kreidenweis, S. M., and Robinson, A. L.: Chemical and physical transformations of organic aerosol from the photo-oxidation of open biomass burning emissions in an environmental chamber, Atmos. Chem. Phys., 11, 7669-7686, https://acp.copernicus.org/articles/11/7669/2011/, 2011.
Holmbom, B.: Improved gas chromatographic analysis of fatty and resin acid mixtures with special reference to tall oil, J. Am. Oil Chem. Soc., 54, 289-293, https://aocs.onlinelibrary.wiley.com/doi/abs/10.1007/BF02671098, 1977.
Huang, R. J., Zhang, Y., Bozzetti, C., Ho, K. F., Cao, J. J., Han, Y., Daellenbach, K. R., Slowik, J. G., Platt, S. M., Canonaco, F., Zotter, P., Wolf, R., Pieber, S. M., Bruns, E. A., Crippa, M., Ciarelli, G., Piazzalunga, A., Schwikowski, M., Abbaszade, G., Schnelle-Kreis, J., Zimmermann, R., An, Z., Szidat, S., Baltensperger, U., El Haddad, I., and Prevot, A. S.: High secondary aerosol contribution to particulate pollution during haze events in China, Nature, 514, 218-222, https://www.ncbi.nlm.nih.gov/pubmed/25231863, 2014.
Kong, X., Salvador, C. M., Carlsson, S., Pathak, R., Davidsson, K. O., Le Breton, M., Gaita, S. M., Mitra, K., Hallquist, A. M., Hallquist, M., and Pettersson, J. B. C.: Molecular characterization and optical properties of primary emissions from a residential wood burning boiler, Sci Total Environ, 754, 142143, https://www.ncbi.nlm.nih.gov/pubmed/32898781, 2021.
Kumar, V., Giannoukos, S., Haslett, S. L., Tong, Y., Singh, A., Bertrand, A., Lee, C. P., Wang, D. S., Bhattu, D., Stefenelli, G., Dave, J. S., Puthussery, J. V., Qi, L., Vats, P., Rai, P., Casotto, R., Satish, R., Mishra, S., Pospisilova, V., Mohr, C., Bell, D. M., Ganguly, D., Verma, V., Rastogi, N., Baltensperger, U., Tripathi, S. N., Prévôt, A. S. H., and Slowik, J. G.: Highly time-resolved chemical speciation and source apportionment of organic aerosol components in Delhi, India, using extractive electrospray ionization mass spectrometry, Atmos. Chem. Phys., 22, 7739-7761, https://acp.copernicus.org/articles/22/7739/2022/, 2022.
Li, C.-T., Zhuang, H.-K., Hsieh, L.-T., Lee, W.-J., and Tsao, M.-C.: PAH emission from the incineration of three plastic wastes, Environ. Int., 27, 61-67, https://www.sciencedirect.com/science/article/pii/S0160412001000563, 2001.
Li, X., Wang, S., Duan, L., Hao, J., Li, C., Chen, Y., and Yang, L.: Particulate and Trace Gas Emissions from Open Burning of Wheat Straw and Corn Stover in China, Environ. Sci. Technol., 41, 6052-6058, https://doi.org/10.1021/es0705137, 2007.
Li, Y.-C. and Kuo, Y.-H.: Labdane-type diterpenoids from the wood of Cunninghamia konishii, Chemical & pharmaceutical bulletin, 50, 498-500, https://doi.org/10.1248/cpb.50.498, 2002.
Liang, Y., Jen, C. N., Weber, R. J., Misztal, P. K., and Goldstein, A. H.: Chemical composition of PM2.5 in October 2017 Northern California wildfire plumes, Atmos. Chem. Phys., 21, 5719-5737, https://acp.copernicus.org/articles/21/5719/2021/, 2021.
Løkke, H.: Picein and piceol concentrations in Norway spruce, Ecotoxicology and Environmental Safety, 19, 301-309, https://www.sciencedirect.com/science/article/pii/014765139090032Z, 1990.
Lopez-Hilfiker, F. D., Pospisilova, V., Huang, W., Kalberer, M., Mohr, C., Stefenelli, G., Thornton, J. A., Baltensperger, U., Prevot, A. S. H., and Slowik, J. G.: An extractive electrospray ionization time-of-flight mass spectrometer (EESI-TOF) for online measurement of atmospheric aerosol particles, Atmos. Meas. Tech., 12, 4867-4886, https://doi.org/10.5194/amt-12-4867-2019, 2019.

https://doi.org/10.5194/egusphere-2023-1102
Preprint. Discussion started: 30 May 2023

Lopez-Hilfiker, F. D., Mohr, C., Ehn, M., Rubach, F., Kleist, E., Wildt, J., Mentel, T. F., Lutz, A., Hallquist, M., Worsnop, D., and Thornton, J. A.: A novel method for online analysis of gas and particle composition: description and evaluation of a Filter Inlet for Gases and AEROsols (FIGAERO), Atmos. Meas. Tech., 7, 983-1001, https://amt.copernicus.org/articles/7/983/2014/, 2014.
Mann, H. B. and Whitney, D. R.: On a test of whether one of two random variables is stochastically larger than the other, Annals of Mathematical Statistics, 18, 50-60, https://doi.org/10.1214/aoms/1177730491, 1947.
Mofikoya, O. O., Mäkinen, M., and Jänis, J.: Chemical Fingerprinting of Conifer Needle Essential Oils and Solvent Extracts by Ultrahigh-Resolution Fourier Transform Ion Cyclotron Resonance Mass Spectrometry, ACS Omega, 5, 10543-10552, https://doi.org/10.1021/acsomega.0c00901, 2020.
Mohr, C., DeCarlo, P. F., Heringa, M. F., Chirico, R., Slowik, J. G., Richter, R., Reche, C., Alastuey, A., Querol, X., Seco, R., Peñuelas, J., Jiménez, J. L., Crippa, M., Zimmermann, R., Baltensperger, U., and Prévôt, A. S. H.: Identification and quantification of organic aerosol from cooking and other sources in Barcelona using aerosol mass spectrometer data, Atmos. Chem. Phys., 12, 1649-1665, https://acp.copernicus.org/articles/12/1649/2012/, 2012.
Neves, L., Ferreira, V., and Oliveira, R.: Co-composting cow manure with food waste: The influence of lipids content, https://doi.org/10.1016/j.biortech.2008.10.030, 2009a.
Neves, L., Oliveira, R., and Alves, M. M.: Fate of LCFA in the co-digestion of cow manure, food waste and discontinuous addition of oil, Water Res., 43, 5142-5150, https://www.sciencedirect.com/science/article/pii/S0043135409005168, 2009b.
Ng, N. L., Canagaratna, M. R., Zhang, Q., Jimenez, J. L., Tian, J., Ulbrich, I. M., Kroll, J. H., Docherty, K. S., Chhabra, P. S., Bahreini, R., Murphy, S. M., Seinfeld, J. H., Hildebrandt, L., Donahue, N. M., DeCarlo, P. F., Lanz, V. A., Prévôt, A. S. H., Dinar, E., Rudich, Y., and Worsnop, D. R.: Organic aerosol components observed in Northern Hemispheric datasets from Aerosol Mass Spectrometry, Atmos. Chem. Phys., 10, 4625-4641, https://acp.copernicus.org/articles/10/4625/2010/, 2010.
Qi, L., Bozzetti, C., Corbin, J. C., Daellenbach, K. R., El Haddad, I., Zhang, Q., Wang, J., Baltensperger, U., Prevot, A. S. H., Chen, M., Ge, X., and Slowik, J. G.: Source identification and characterization of organic nitrogen in atmospheric aerosols at a suburban site in China, Sci Total Environ, 818, 151800, https://www.ncbi.nlm.nih.gov/pubmed/34813816, 2022.
Radke, L. and Ward, D., Crutzen, P. J., and Goldammer, J. G. (Eds.): The Ecological, Atmospheric, and Climatic Importance of Vegetation Fires., Environmental Sciences Research Report, John Wiley and Sons, Inc., New York, pp.1993.
Rugiel, M. M., Setkowicz, Z. K., Drozdz, A. K., Janeczko, K. J., Kutorasińska, J., and Chwiej, J. G.: The Use of Fourier Transform Infrared Microspectroscopy for the Determination of Biochemical Anomalies of the Hippocampal Formation Characteristic for the Kindling Model of Seizures, ACS Chem. Neurosci., 12, 4564-4579, https://doi.org/10.1021/acschemneuro.1c00642, 2021.
Saiz-Jimenez, C. and De Leeuw, J. W.: Lignin pyrolysis products: Their structures and their significance as biomarkers, Org. Geochem., 10, 869-876, https://www.sciencedirect.com/science/article/pii/S0146638086800249, 1986.
Simoneit, B. R. T.: Biomass burning — a review of organic tracers for smoke from incomplete combustion, Appl. Geochem., 17, 129-162, https://www.sciencedirect.com/science/article/pii/S0883292701000610, 2002.
Simoneit, B. R. T., Rogge, W. F., Mazurek, M. A., Standley, L. J., Hildemann, L. M., and Cass, G. R.: Lignin pyrolysis products, lignans, and resin acids as specific tracers of plant classes in emissions from biomass combustion, Environ. Sci. Technol., 27, 2533-2541, https://doi.org/10.1021/es00048a034, 1993.
Smith, K. R., Bruce, N., Balakrishnan, K., Adair-Rohani, H., Balmes, J., Chafe, Z., Dherani, M., Hosgood, H. D., Mehta, S., Pope, D., and Rehfuess, E.: Millions Dead: How Do We Know and What Does It Mean? Methods Used in the Comparative Risk Assessment of Household Air Pollution, Annu. Rev. Public Health, 35, 185-206, https://www.annualreviews.org/doi/abs/10.1146/annurev-publhealth-032013-182356, 2014.
Stark, H., Yatavelli, R. L. N., Thompson, S. L., Kang, H., Krechmer, J. E., Kimmel, J. R., Palm, B. B., Hu, W., Hayes, P. L., Day, D. A., Campuzano-Jost, P., Canagaratna, M. R., Jayne, J. T., Worsnop, D. R., and Jimenez, J. L.: Impact of Thermal Decomposition on Thermal Desorption Instruments: Advantage of Thermogram Analysis for Quantifying Volatility Distributions of Organic Species, Environ Sci Technol, 51, 8491-8500, https://www.ncbi.nlm.nih.gov/pubmed/28644613, 2017.
Stockwell, C. E., Christian, T. J., Goetz, J. D., Jayarathne, T., Bhave, P. V., Praveen, P. S., Adhikari, S., Maharjan, R., DeCarlo, P. F., Stone, E. A., Saikawa, E., Blake, D. R., Simpson, I. J., Yokelson, R. J., and Panday, A. K.: Nepal Ambient Monitoring and Source Testing Experiment (NAMaSTE): emissions of trace gases and light-absorbing carbon from wood and dung cooking fires, garbage and crop residue burning, brick kilns, and other sources, Atmos. Chem. Phys., 16, 11043-11081, https://acp.copernicus.org/articles/16/11043/2016/, 2016.
Surdu, M., Lamkaddam, H., Wang, D. S., Bell, D. M., Xiao, M., Lee, C. P., Li, D., Caudillo, L., Marie, G., Scholz, W., Wang, M., Lopez, B., Piedehierro, A. A., Ataei, F., Baalbaki, R., Bertozzi, B., Bogert, P., Brasseur, Z., Dada, L., Duplissy, J., Finkenzeller, H., He, X. C., Hohler, K., Korhonen, K., Krechmer, J. E., Lehtipalo, K., Mahfouz,

https://doi.org/10.5194/egusphere-2023-1102
Preprint. Discussion started: 30 May 2023

N. G. A., Manninen, H. E., Marten, R., Massabo, D., Mauldin, R., Petaja, T., Pfeifer, J., Philippov, M., Rorup, B., Simon, M., Shen, J., Umo, N. S., Vogel, F., Weber, S. K., Zauner-Wieczorek, M., Volkamer, R., Saathoff, H., Mohler, O., Kirkby, J., Worsnop, D. R., Kulmala, M., Stratmann, F., Hansel, A., Curtius, J., Welti, A., Riva, M., Donahue, N. M., Baltensperger, U., and El Haddad, I.: Molecular Understanding of the Enhancement in Organic Aerosol Mass at High Relative Humidity, Environ Sci Technol, 57, 2297-2309, https://www.ncbi.nlm.nih.gov/pubmed/36716278, 2023.

Szmigielski, R., Surratt, J. D., Gómez-González, Y., Van der Veken, P., Kourtchev, I., Vermeylen, R., Blockhuys, F., Jaoui, M., Kleindienst, T. E., Lewandowski, M., Offenberg, J. H., Edney, E. O., Seinfeld, J. H., Maenhaut, W., and Claeys, M.: 3-methyl-1,2,3-butanetricarboxylic acid: An atmospheric tracer for terpene secondary organic aerosol, Geophys. Res. Lett., 34, https://agupubs.onlinelibrary.wiley.com/doi/abs/10.1029/2007GL031338, 2007.

Tai, K. Y., Dhaliwal, J., and Balasubramaniam, V.: Leveraging Mann–Whitney U test on large-scale genetic variation data for analysing malaria genetic markers, Malar. J., 21, 79, https://doi.org/10.1186/s12936-022-04104-x, 2022.

Tobler, A., Bhattu, D., Canonaco, F., Lalchandani, V., Shukla, A., Thamban, N. M., Mishra, S., Srivastava, A. K., Bisht, D. S., Tiwari, S., Singh, S., Močnik, G., Baltensperger, U., Tripathi, S. N., Slowik, J. G., and Prévôt, A. S. H.: Chemical characterization of PM2.5 and source apportionment of organic aerosol in New Delhi, India, Sci. Total Environ., 745, 140924, https://www.sciencedirect.com/science/article/pii/S0048969720344533, 2020.

Tong, Y., Pospisilova, V., Qi, L., Duan, J., Gu, Y., Kumar, V., Rai, P., Stefenelli, G., Wang, L., Wang, Y., Zhong, H., Baltensperger, U., Cao, J., Huang, R. J., Prévôt, A. S. H., and Slowik, J. G.: Quantification of solid fuel combustion and aqueous chemistry contributions to secondary organic aerosol during wintertime haze events in Beijing, Atmos. Chem. Phys., 21, 9859-9886, https://acp.copernicus.org/articles/21/9859/2021/, 2021.

Tuet, W. Y., Liu, F., de Oliveira Alves, N., Fok, S., Artaxo, P., Vasconcellos, P., Champion, J. A., and Ng, N. L.: Chemical Oxidative Potential and Cellular Oxidative Stress from Open Biomass Burning Aerosol, Environ. Sci. Technol. Lett., 6, 126-132, https://doi.org/10.1021/acs.estlett.9b00060, 2019.

Wang, Y., Wang, Q., Ye, J., Yan, M., Qin, Q., Prévôt, A. S. H., and Cao, J.: A Review of Aerosol Chemical Composition and Sources in Representative Regions of China during Wintertime, Atmosphere, 10, 277, https://www.mdpi.com/2073-4433/10/5/277, 2019.

Ward, D. E. and Hardy, C. C.: Smoke emissions from wildland fires, Environ. Int., 17, 117-134, https://www.sciencedirect.com/science/article/pii/0160412091900958, 1991.

Wilcoxon, F.: Individual Comparisons by Ranking Methods, Biometrics Bulletin, 1, 80-83, http://www.jstor.org/stable/3001968, 1945.

Wiyono, B., Tachibana, S., and Tinambunan, D.: Chemical Compositions of Pine Resin, Rosin and Turpentine Oil from West Java, Indonesian Journal of Forestry Research, 3, 7-17, http://doi.org/10.20886/ijfr.2006.3.1.7-17, 2006.

Xu, W., He, Y., Qiu, Y., Chen, C., Xie, C., Lei, L., Li, Z., Sun, J., Li, J., Fu, P., Wang, Z., Worsnop, D. R., and Sun, Y.: Mass spectral characterization of primary emissions and implications in source apportionment of organic aerosol, Atmos. Meas. Tech., 13, 3205-3219, https://amt.copernicus.org/articles/13/3205/2020/, 2020.

Yee, L. D., Kautzman, K. E., Loza, C. L., Schilling, K. A., Coggon, M. M., Chhabra, P. S., Chan, M. N., Chan, A. W. H., Hersey, S. P., Crounse, J. D., Wennberg, P. O., Flagan, R. C., and Seinfeld, J. H.: Secondary organic aerosol formation from biomass burning intermediates: phenol and methoxyphenols, Atmos. Chem. Phys., 13, 8019-8043, https://acp.copernicus.org/articles/13/8019/2013/, 2013.

https://doi.org/10.5194/egusphere-2023-1102
Preprint. Discussion started: 30 May 2023

Tables and figures

Table 1 Average emission factors of CO, CO_2, THC, PM, OM, and BC as well as MCE for 6 types of burning.

Burning type	Carbon content	MCE	Emission factors (g kg^{-1} fuel)					
			CO	CO_2	THC	PM	OM	eBC*
beech logs stove (n=5)	0.46	0.91±0.03	85.8±25.9	1466.9±65.8	19.3±5.5	7.6±2.2	6.2±2.8	2.43±0.9
spruce and pine logs stove (n=8)	0.46	0.91±0.02	83.8±26.7	1640.7±58	16.1±4.8	4.9±2.2	2.0±1.3	n.a
spruce and pine branches and needles open (n=4)	0.46	0.93±0.02	63.5±6.8	1668.9±26.7	14.1±3.4	9.4±2.7	3.8±1.1	n.a
straw open (n=6)	0.45	0.95±0.04	44.4±34.1	1511.7±103.2	19.1±17	2.8±1.2	2.4±1.3	0.7±0.2
cow dung open (n=6)	0.45	0.87±0.03	92.3±27.4	1366.2±88.4	30.3±8.5	16.6±10.8	16.2±10.8	0.8±0.3
plastic bags open (n=4)	0.84	0.98±0.02	29.3±39.2	2956.6±138.9	18.2±28.6	3.1±1.3	1.3±0.3	1.0±0.3

* The number of burns is indicated by n. BC data is not available for some burns.

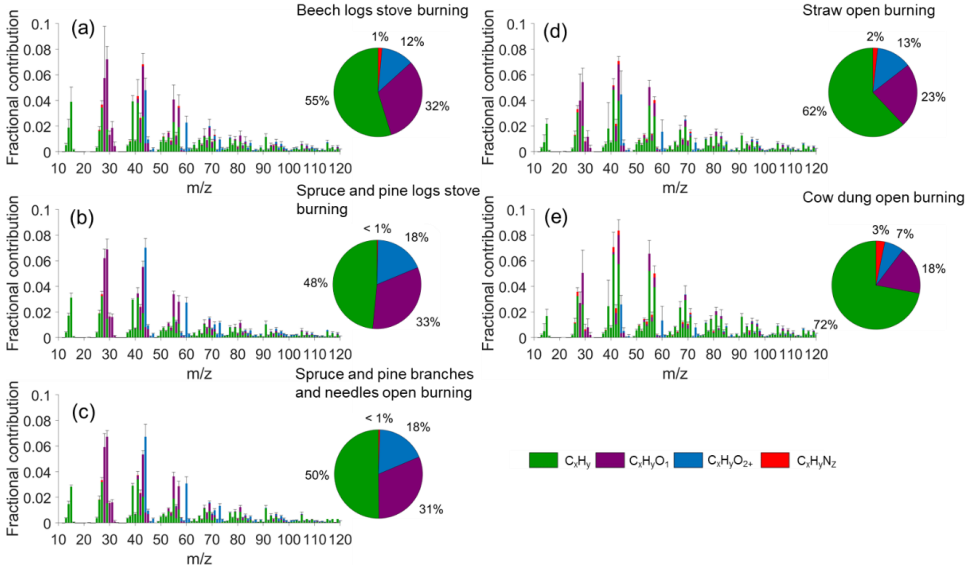

Figure 1 Average AMS POA mass spectral profiles and elemental compositions of (a) beech logs stove burning (n=6; n is the number of experiments), (b) spruce and pine logs stove burning (n=9), (c) spruce and pine branches and needles open burning (n=4), (d) straw open burning (n=6), and (e) cow dung open burning (n=5). The error bar denotes half standard deviation in grey. The pie chart showing the contribution of elemental families is at the right of the mass spectrum.

https://doi.org/10.5194/egusphere-2023-1102
Preprint. Discussion started: 30 May 2023

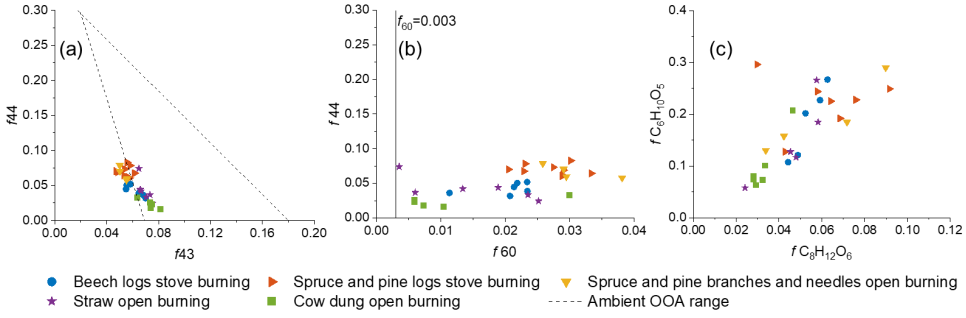

Figure 2. Scatter plots of (a) f_{44} vs. f_{43} from AMS, (b) f_{44} vs. f_{60} from AMS, and (c) $f C_6H_{10}O_5$ vs. $f C_8H_{12}O_6$ from EESI-TOF. The dashed line denotes the estimated OOA range and the solid line denotes f_{60} background level in the ambient from Ng et al. (2010) and Cubison et al. (2011).

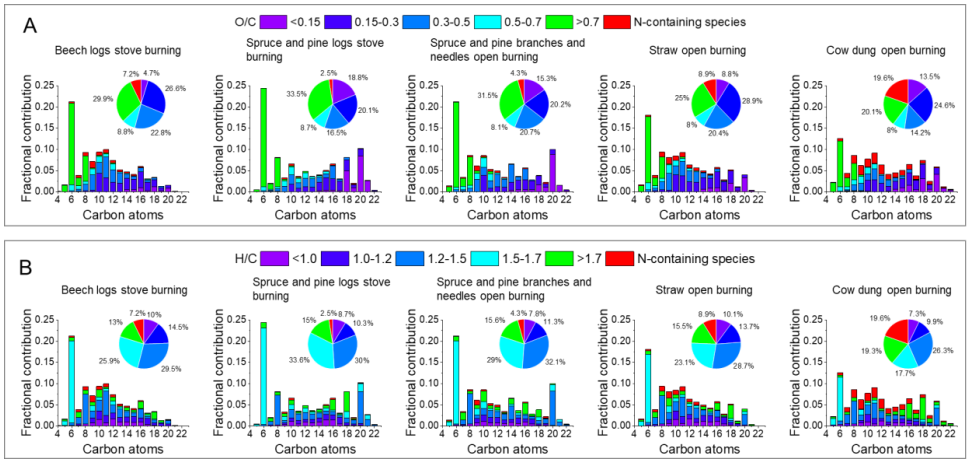

Figure 3 The average carbon and oxygen distribution colored by the O/C and H/C for non-N-containing species in panel A and B respectively with EESI-TOF. The N-containing species are colored in red. The pie charts are the corresponding contribution of a range of O/C or H/C ratios.

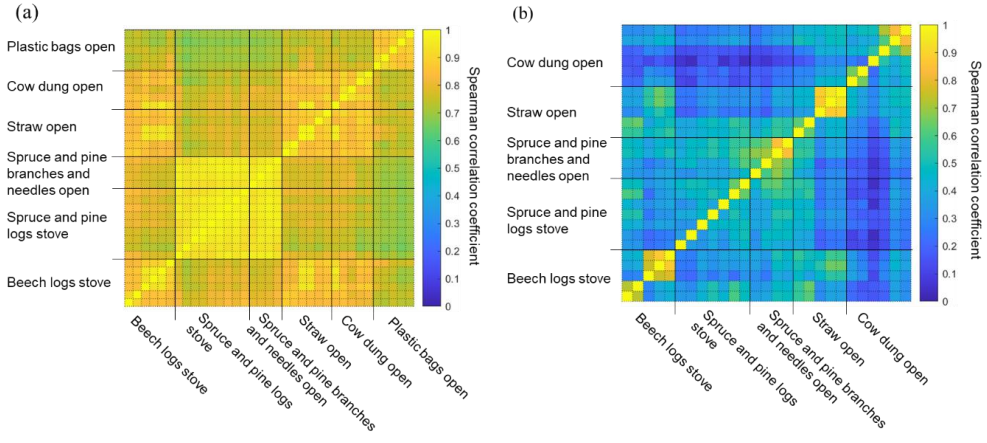

Figure 4 The correlation matrix of POAs measured with (a) the HR data from AMS and (b) EESI-TOF using Spearman correlation function. Note that some experiments did not have either AMS or EESI-TOF data.

https://doi.org/10.5194/egusphere-2023-1102
Preprint. Discussion started: 30 May 2023

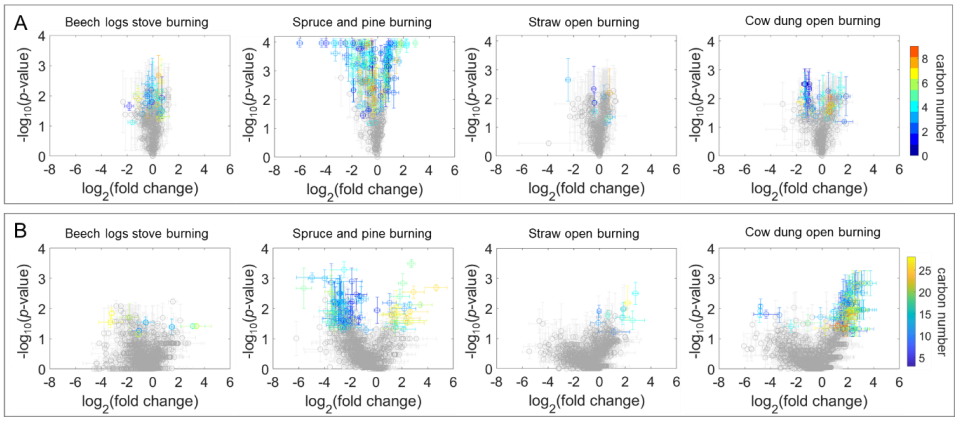

Figure 5 The static *p*-value vs. fold change with the dataset from AMS in panel A and EESI-TOF in panel B. The color bars are the number of carbon atoms. The horizontal error bars are the 1 standard deviation given by the *p*-value variations in the pairwise tests, and the vertical error bars are the 1 standard deviation of the log_2(fold change).

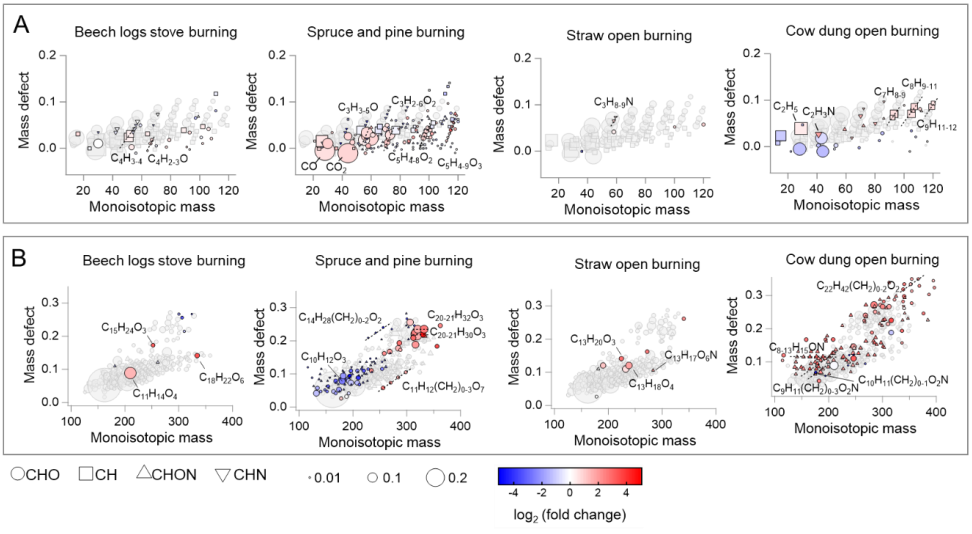

Figure 6 The mass defect plot with the dataset from AMS in panel A and EESI-TOF in panel B. The markers denotes the fragments or molecules having the same formula. They are sized by the square root of fractional contribution and colored by the log_2(fold change).